American Mineralogist, Volume 95, pages 968–973, 2010

Silicon coordination in rutile and TiO_2-II at ambient and high pressures: Si-29 NMR

Jed L. Mosenfelder,[1] Namjun Kim,[2] and Jonathan F. Stebbins[2,*]

[1]Division of Geological and Planetary Sciences, California Institute of Technology, M/C 170-25, Pasadena, California 91125-2500, U.S.A.
[2]Department of Geological and Environmental Sciences, Stanford University, Stanford, California 94305, U.S.A.

Abstract

The structural environment of silicon dissolved in rutile and α-PbO_2-structured TiO_2 (TiO_2-II) was probed using ^{29}Si MAS NMR on ^{29}Si-enriched samples. At 1 atm, about 0.01 wt% SiO_2 is incorporated into TiO_2 as ^{IV}Si, presumably in interstitial sites. Rutile recovered from 6 GPa, 1600 °C contains about 0.6 wt% SiO_2, incorporated both as ^{VI}Si (~90%) and ^{IV}Si (~10%). TiO_2-II, synthesized at 12 GPa, 1200 °C, contains only ^{VI}Si. The chemical shift for ^{VI}Si in TiO_2-II is slightly less negative than that for rutile, and the peak is split, suggesting either a more complex mechanism of substitution or a different response to quenching or decompression in the lower-symmetry structure. Future thermodynamic studies of the TiO_2-SiO_2 solid solution will have to take into account the mixed coordination environment of the Si in TiO_2, at low pressures.

Keywords: Crystal structure, rutile, TiO_2-II, high-pressure studies, NMR spectroscopy

Introduction

The solubility of SiO_2 in the various polymorphs of TiO_2, and the mechanism of incorporation of the dissolved Si, are of interest both for high-pressure petrology and for technological materials. The fact that stishovite (stable above about 9 GPa at mantle temperatures) is isostructural with rutile suggests that there should be significant solid solution at high pressures, which could in principle be used as a geothermobarometer (Stebbins 1992; Vinograd et al. 2008; Ren et al. 2009). At least at lower pressures, where the stable silica polymorph is coesite or quartz, there could be a strong pressure effect on solubility, given the expected large negative molar volume change on transition from tetrahedral (^{IV}Si) to octahedral (^{VI}Si) silicon coordination. Such an effect can be seen in the study of Gaetani et al. (2008) on rutile solubility in silicate melts; their data on SiO_2 concentrations in the rutile coexisting with rhyodacitic or haplobasaltic melts (Fig. 1) reveal a systematic increase from about 0.06 to 0.3 wt% SiO_2 with pressure increasing from 1 atm to 3.5 GPa. This raises the possibility that Si in rutile could be used as a "probe" to estimate the amount of ^{VI}Si in high-pressure melts, if the thermodynamics and structure of the substitution were well constrained.

Reports of high concentrations of Si in natural rutiles are scant in the literature. A comprehensive survey of rutiles from high (>1 GPa) to ultra-high pressure (UHP) (up to 4.5 GPa) rocks by Zack et al. (2004) yielded typical concentrations of only ~100 wt ppm, with a maximum of 929 ppm, as measured by laser-ablation ICP-MS. On the other hand, Schulze (1990) reported SiO_2 contents of 0.25–0.29 wt% for massive rutile in nodules from the Kampfersdam and Kimberley kimberlite pipes in South Africa. Mposkos and Kostopoulos (2001) measured 0.43 wt% SiO_2 in a rutile inclusion in garnet from the Rhodope UHP province in Greece. Finally—and most spectacularly—Yang et al. (2003) measured concentrations of 11–15 wt% SiO_2 in rutile from a chromitite in the Luobusa ophiolite in Tibet, apparently metamorphosed under UHP conditions (Yang et al. 2007).

This last report motivated an experimental study of Si solubility in TiO_2 as a function of pressure and temperature (Ren et al. 2009). The experiments were conducted in the stability fields of rutile and its high-pressure polymorph, α-PbO_2-structured TiO_2 (or TiO_2-II), and possibly even into the stability field of the still higher-pressure baddeleyite-structured polymorph. These authors found SiO_2 contents in TiO_2—coexisting with coesite or stishovite—ranging from a few tenths of 1 wt% at 1500 °C to a maximum of about 5 wt% at 2000 °C and 23 GPa.

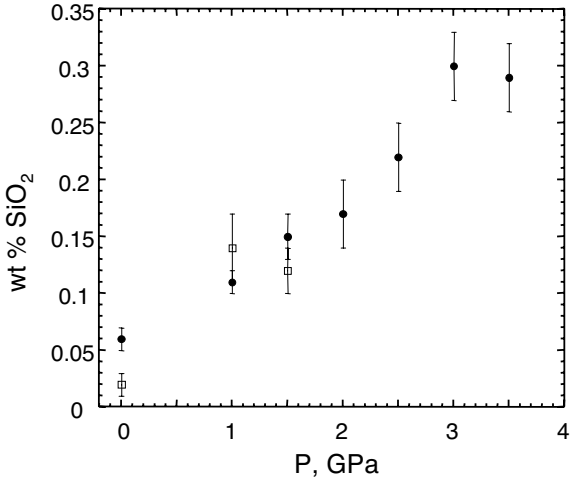

Figure 1. SiO_2 content of rutile coexisting with rhyodacitic melt (closed circles) or haplobasaltic melt (open squares) at 1350 °C, from experiments of Gaetani et al. (2008), showing systematic increase with pressure.

* E-mail: stebbins@stanford.edu

0003-004X/10/0007–968$05.00/DOI: 10.2138/am.2010.3491

The data demonstrate very strong increases in solubility with temperature and a moderately strong pressure effect at higher temperatures. Density functional theory calculations were found to be generally consistent with these results, at least for rutile coexisting with coesite (Vinograd et al. 2008). Given the known structures of rutile and stishovite, these studies only considered the presence of ^{VI}Si.

Titania in the form of anatase and rutile is important in technologies including catalysts, ceramics, pigments, photovoltaics, and other materials. Minor elements can have major effects on their properties. In particular, added silica can retard the transition from anatase to rutile on heating by as much as 200 °C, which has led to several studies attempting to elucidate the microstructural nature of this solid solution (Akhtar et al. 1992; Yoshinaka et al. 1997; Okada et al. 2001). Indirect evidence for both ^{IV}Si and ^{VI}Si has been presented for low-temperature synthetic anatase purportedly containing as much as 15 wt% SiO_2. In contrast, few structural studies of Si in rutile have been reported (Stebbins 1992), and the silica solubility in this high-temperature phase is thought to be much lower, despite the structural similarities of anatase and rutile (Smyth and Bish 1988).

In this preliminary study, we present some of the first clear evidence for the coordination number of Si dissolved in ambient- and high-pressure TiO_2 phases, as well as constraints on at least minimum silica contents in titania in the presence of cristobalite, coesite, or stishovite.

Experimental methods

Sample synthesis and characterization

TiO_2 (99.999% purity, Sigma-Aldrich, as rutile) was ground in an agate mortar with 2.1 wt% of 99.4% ^{29}Si-enriched silica (Isonics), then heated in air at 1500 °C for a total of 160 h, with two intermediate grinding steps. Two high-pressure experiments were conducted in a Walker-style multi-anvil apparatus with this starting material, one at 6 GPa, 1600 °C, for 24 h and one at 12 GPa, 1200 °C, for 8 h. For the 6 GPa synthesis, we loaded 80 mg of powder into a Pt capsule (3.8 mm diameter, 4 mm length) that was welded shut after drying at 125 °C and inserted into a 25/15 assembly with a $LaCrO_3$ heater (Kelsey et al. 2009). The 12 GPa synthesis used 68 mg of powder, packed into a folded foil Pt capsule (3.5 mm diameter, 3.4 mm length, dried at 125 °C but not welded) and inserted into a 14/8 G2 assembly with a graphite furnace (Leinenweber et al. 2006). Temperature was measured using type C thermocouples, separated from the capsules by a 0.3 mm thick disk of hard alumina. The 6 GPa run was quenched rapidly by turning off power to the furnace; unfortunately, the 12 GPa run was terminated abruptly after almost exactly 8 h at 1200 °C by conversion of the graphite to diamond.

Powder X-ray diffraction data showed the presence only of rutile (plus coesite) in the 6 GPa sample and of TiO_2-II (plus stishovite) in the 12 GPa sample. During both high-pressure runs, the initially light yellowish-brown rutile became dark blue in color. This phenomenon is typical for high-pressure synthetic rutile and is caused by intervalence charge transfer between Ti^{3+} and Ti^{4+}, with trace amounts of Ti^{3+} formed by reducing conditions (Khomenko et al. 1998). After initial NMR spectra were recorded, each sample was annealed in air at 240 °C for 2 h, restoring the color to light gray, indicating re-oxidation to Ti^{4+}. The annealing conditions were chosen based on previous work (McQueen et al. 1967; Khomenko et al. 1998), to achieve re-oxidation to Ti^{4+} without reversion to rutile (in the case of TiO_2-II) and without changing the coordination state of Si in rutile.

Electron microprobe analyses (EPMA) (Table 1) were obtained using a JEOL JXA-8200 on small fragments of the recovered samples that were mounted in epoxy, polished, and measured using the same standards and operating conditions outlined by Mosenfelder et al. (2006).

NMR spectroscopy

MAS NMR spectra were collected with a Varian Infinity 400 spectrometer (9.4 Tesla, 79.4 MHz), using a 3.2 mm probe, zirconia rotors, and spinning rates of 11 kHz. Sample weights ranged from about 40 to 70 mg. Single-pulse acquisition was used with 0.7 µs pulses (30° radiofrequency tip angle), with tetramethylsilane (TMS) as the frequency reference. Data were acquired with pulse delays from 1 s to 3600 or 5400 s to determine effects of relaxation, with the total acquisition time for each spectrum typically at least 24 h. Spectra of synthetic forsterite (natural isotopic abundance) collected with a 3600 s pulse delay (fully relaxed) were used to calibrate observed peak areas (Stebbins et al. 2009). Reported chemical shifts have uncertainties of about ±0.1 ppm.

Results

Ambient-pressure rutile

For all NMR spectra of the 1 bar starting material, the predominant peak is for cristobalite (Fig. 2). Its mean chemical shift (–110.0 ppm) is slightly lower than that typically seen for high-purity cristobalite, and its width (FWHM = 2.4 ppm) considerably broader (Smith and Blackwell 1983; Spearing et al. 1992; Phillips et al. 1993). Both of these effects were seen in an earlier study of Si in rutile (Stebbins 1992). A narrower, unshifted peak was reported in that study for cristobalite equilibrated with 1% titania, suggesting that dissolved TiO_2 is not the source of the broadening. Stacking faults (tridymite-like layers) may produce non-ideal spectra of cristobalite (Phillips et al. 1993); interactions with the surfaces of rutile particles have also been suggested (Stebbins 1992). At the signal-to-noise ratio (S/N) obtainable at the longest pulse delay used (3600 s), this peak is the only visible feature. Its calibrated peak area corresponds to 1.4 wt% SiO_2 (vs. 2.1% nominal), suggesting that even at this long delay its signal is not fully relaxed. This is a common problem for silica polymorphs, which exclude from their structures the paramagnetic transition metal cations that are primarily responsible for spin-lattice relaxation (MacKenzie and Smith 2002).

At shorter delays, with correspondingly greater numbers of acquisitions and higher S/N for more rapidly relaxing resonances, a much smaller, narrow peak becomes visible at –77.3 ppm (Fig. 2, top spectrum). This corresponds precisely to previously published data for another sample of $^{29}SiO_2$-doped rutile, which was collected with a different probe and rotor (Stebbins 1992). Although noisy, spectra collected with pulse delays of 60–120 s suggest that this is nearly fully relaxed. Scaled to the estimated fully relaxed intensity for the cristobalite, the area of this peak corresponds to about 0.01 wt% SiO_2 in the rutile, presumably in a tetrahedral interstitial defect site. This concentration is much lower than the previous estimate (Stebbins 1992), however, as the latter was based on an unrelaxed intensity for the cristobalite, not on a relaxed standard spectrum.

6 GPa rutile

The grain size of the recovered material, estimated from back-scattered electron images (showing obvious grain bound-

Table 1. Electron microprobe analyses

Run no.	ww412		ww413		
Conditions	6 GPa, 1600 °C Average analyses		12 GPa, 1200 °C Representative analyses		
	Chip 1	Chip 2	1	2	3
SiO_2	0.78(3)	0.59(3)	0.71	0.57	0.12
TiO_2	99.78(38)	99.86(23)	99.63	99.75	100.2
FeO	0.03(1)	0.01(1)	0.05	0.01	0
MgO	0.03(1)	0.03(1)	0.03	0.03	0.01
Oxide total	100.62(35)	100.48(22)	100.42	100.36	100.33

Notes: Numbers in parentheses represent standard deviation for five analyses (chip 1) or eight analyses (chip 2). Al, Cr, Mn, Ca, Na, K, P, and Ni were also analyzed, but all were below the detection limit (0.02 wt% or less).

aries as cracks), was about 50–100 μm. EPMA analyses (Table 1) were obtained on two different polycrystalline fragments of the sample, placed in the same epoxy mount and analyzed in the same session. The two fragments give systematically different SiO_2 concentrations in rutile, 0.78 or 0.59 wt% (measured on multiple grains in each fragment; see Table 1). One possibility for this difference is that the two fragments came from distinctly different portions of the sample that were in different portions of a temperature gradient, but such spatial information was not recorded as our main goal was to maximize the volume of material for NMR spectroscopy. Assuming that the higher Si-content rutile came from the middle of the capsule (at higher temperature, farther from the thermocouple), we therefore crudely estimate the minimum SiO_2 solubility to be 0.6 wt% at 1600 °C, 6 GPa.

Long-delay NMR spectra for this sample contain the doublet of peaks for the two distinct Si sites in coesite (–108.3 ppm, –114.0 ppm) as reported previously (Smith and Blackwell 1983), as expected for the excess silica phase at this pressure. In the original, unannealed (dark blue) sample, an additional small peak was observed at –177.5 ppm, corresponding to octahedrally coordinated Si (^{VI}Si) in the rutile. After annealing in air at 240 °C for 2 h, the intensity of the latter grew by more than an order of magnitude. Further annealing (240 °C, 18 h) did not result in a further increase. As in the ambient-pressure sample, the NMR signal from the 6 GPa rutile relaxed much more rapidly than that for the pure silica phase, probably because of trace levels of paramagnetic impurities. At relatively short pulse delays (e.g., 60 s), high enough S/N could be obtained to also detect a small ^{IV}Si peak at the same position as in the 1 bar sample. Its area is about 10% of that for the ^{VI}Si; this ratio does not appear to change with pulse delay, supporting its presence in the same phase as the ^{VI}Si. The observed ^{IV}Si/^{VI}Si ratio was not significantly increased after the second, longer annealing, suggesting that the ^{IV}Si is inherent in the high-pressure rutile and not a product of local structural relaxation during this mild re-heating at 1 bar.

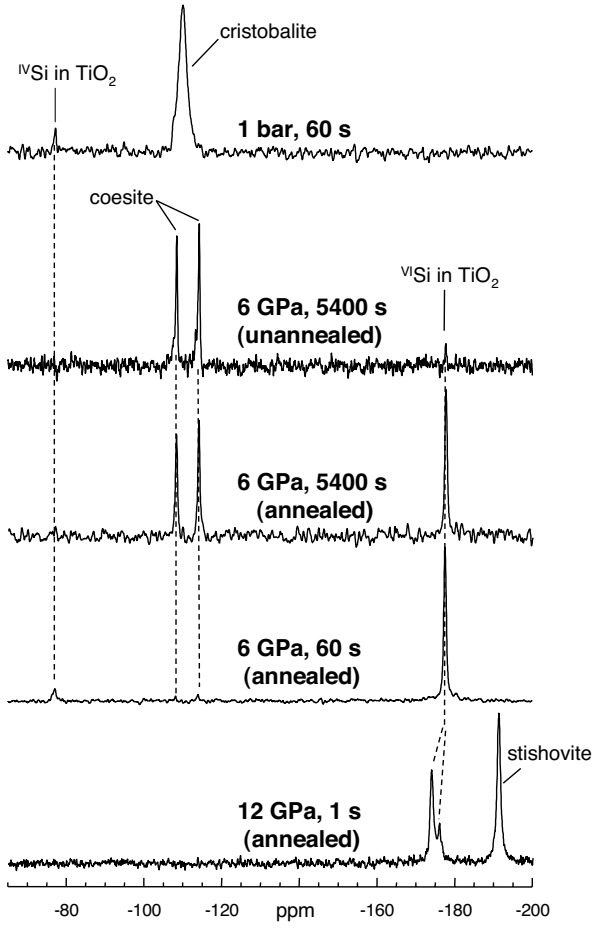

FIGURE 2. Representative ^{29}Si MAS NMR of TiO_2 samples containing dissolved silica. Synthesis pressures and NMR pulse delays are shown. Top four spectra are for rutile, lowermost is for TiO_2-II. Intensities of spectra are normalized to the highest peak in each.

The low intensity of the peaks for Si in the unannealed 6 GPa rutile are likely to result from effects of the unpaired electron spins on the Ti^{3+} cations, which are mitigated by conversion back to Ti^{4+} during annealing. Such paramagnetic impurities can shift and/or broaden NMR resonances, either through bulk magnetic susceptibility effects, "contact shift" mechanisms, and/or by generating extremely short relaxation times (Grey et al. 1990; Hartman et al. 2007; Stebbins and Kelsey 2009). The rapidity of the changes in color and NMR response on annealing at only 240 °C suggest that the removal of paramagnetic centers is not controlled by the simple diffusion of oxygen into the bulk crystal powders, which is too slow given the grain size of about 50 to 100 μm (Moore et al. 1998). A more likely mechanism is diffusion of trace amounts of hydrogen out of the grains (Khomenko et al. 1998), which is much more kinetically favorable at this temperature (Johnson et al. 1975).

For the annealed 6 GPa sample, integration of all peaks in the longest-delay spectrum (5400 s) yields an estimated total of 0.73 wt% SiO_2, which is well below the nominal content of 2.1% and again suggests that the signal from the pure silica phase is not completely relaxed.

In a systematic study of the relaxation of the rutile ^{VI}Si component, peak heights or areas from spectra with pulse delays from 10 to 5400 s were well fitted by a stretched exponential equation for the magnetization M as a function of relaxation delay τ. This is typical when relaxation is controlled by through-space dipolar coupling between nuclear spins and unpaired electron spins on dilute paramagnetic impurities (Tse and Hartmann 1968; Hartman et al. 2007):

$$M = M_\infty \{1 - \exp[-(\tau/T')^{0.5}]\}.$$

Results (Fig. 3) indicate a relaxation time constant T′ of 67±7 s and full relaxation by 5400 s. Fitting with the same number of adjustable parameters, but a normal exponential function (exponent of 1.0 instead of 0.5, giving a standard "relaxation time" T_1) gives a much worse fit, as demonstrated recently for several silicate minerals (Hartman et al. 2007; Stebbins and Kelsey 2009; Stebbins et al. 2009). Clustering or incomplete dispersion of the isotopically enriched ^{29}Si could be expected to cause rapid nuclear spin diffusion and an exponent closer to 1; our observations thus support the lack of such clustering. The calibrated peak area for the ^{VI}Si, combined with that for the

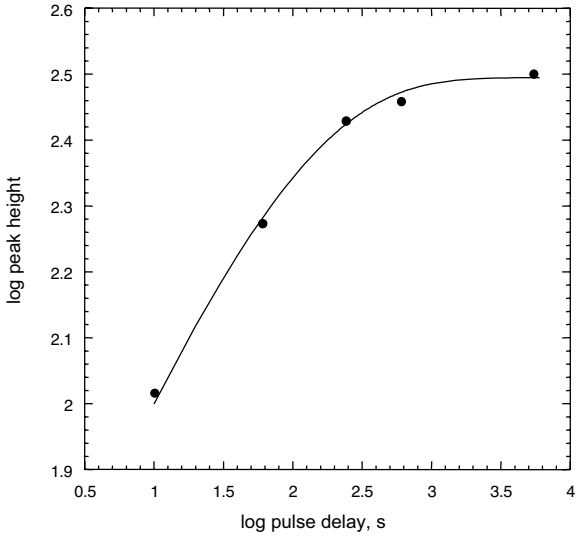

FIGURE 3. Plot of $\log_{10}$ of NMR peak heights vs. $\log_{10}$ of NMR pulse delay for the ^{VI}Si peak in the 6 GPa rutile. The curve shown results from fitting of a stretched exponential relaxation function to the data in linear space to ensure proper weighting of uncertainties (see text).

^{IV}Si, suggests a total dissolved SiO_2 content in the rutile of about 0.3%. The discrepancy between this value and that estimated by EPMA cannot readily be resolved without extensive further studies of response to annealing: for example, if some of the NMR signal is still "masked" by residual Ti^{3+}, the NMR value could be an underestimate.

12 GPa TiO_2-II

Powder XRD detected only the TiO_2-II phase (α-PbO_2 structure) plus stishovite in this sample. This was the expected result, given that the nominal pressure of the experiment was 2.9 GPa higher than the rutile-TiO_2-II boundary (Withers et al. 2003) and that a strong partitioning of Si between the two TiO_2 polymorphs, which could extend the stability field of rutile, is not expected based on available solubility data (Ren et al. 2009). The grain size of this sample was significantly smaller than in the 6 GPa run, about 10 to 30 μm. EPMA analyses on two different fragments of the sample show strong scatter with no obvious systematics, ranging from 0 wt% SiO_2 (not shown in Table 1) to 0.71 wt% SiO_2, the maximum amount measured among 21 analyses. This scatter undoubtedly reflects slower diffusion kinetics for Si in TiO_2 for the lower temperature and duration of this run compared to the 6 GPa experiment (despite the significantly smaller grain size). Nevertheless, the Si coordination environment for the bulk sample could be probed using NMR.

As for the 6 GPa rutile, a 2 h anneal in air at 240 °C removed the dark blue color and greatly improved the NMR spectrum of the dissolved Si. XRD patterns taken before and after annealing on the sample were identical, confirming that no reversion of the high-pressure phase to rutile took place. The stishovite gives a narrow peak at –191.2 ppm, as previously described (Smith and Blackwell 1983; Stebbins and Kanzaki 1990). In the TiO_2-II, ^{VI}Si was again observed, but as a pair of peaks at –174.0 ppm and –176.0 ppm with an area ratio of about 5/1. These chemical shifts are significantly different from that for rutile (–177.5 ± 0.1 ppm). As for the other samples, the total integrated peak area corresponds to a silica content below that of the nominal value (1.4 vs. 2.1 wt%), again probably because fully relaxed spectra for the pure silica phase could not be obtained. The area of the much faster relaxing ^{VI}Si peak corresponds to 0.25 wt% SiO_2 in the TiO_2-II, which reflects the average of concentrations in grains with varying composition, given the EPMA data. No ^{IV}Si peak was observed, at a detection limit of about 3% of the ^{VI}Si signal, indicating that this species clearly has a lower relative abundance than in the 6 GPa rutile.

DISCUSSION

The experiments described here were not designed to demonstrate thermodynamic equilibrium. Rather, we purposely optimized sample volume at the expense of careful control of temperature gradients, to recover sufficient material for high-precision NMR study. However, the estimated silica content of the 6 GPa rutile in the presence of excess coesite, about 0.6 wt%, is roughly consistent with previous experimental studies (Ren et al. 2009) and theoretical calculations (Vinograd et al. 2008). For the 12 GPa, 1200 °C sample of TiO_2-II, the run time and temperature were insufficient for silica to diffuse through the grains, as indicated by the highly heterogeneous EPMA data.

In both high-pressure rutile and TiO_2-II most of the dissolved Si is ^{VI}Si. However, the detection of small amounts of ^{IV}Si in the 1 bar and 6 GPa rutile samples suggests that this species may also need to be considered when analyzing lower-pressure phase equilibria. The reduction to below the detection limit of this species in the 12 GPa sample suggests the possibility of a pressure-dependent internal partitioning between these two types of sites, which could even conceivably prove to be useful in natural samples of SiO_2-saturated TiO_2 phases, although NMR sensitivity issues could make this a difficult task. (Alternatively, the minor differences between the rutile and TiO_2-II structures could affect this partitioning.) The exact nature of ^{IV}Si substitution in titania remains incompletely characterized: tetrahedral interstitial vacancies are indeed present in the structure of rutile, but whether Si substitution is accompanied by the formation of oxygen interstitials as well, by octahedral Ti^{4+} vacancies (more likely), or by another mechanism, is not known. Future application of Si in TiO_2 as a geothermobarometer will not only require consideration of ^{IV}Si solubility but a more extensive set of experiments than those conducted by Ren et al. (2009), particularly at lower pressures and temperatures (and thus lower Si contents).

Several studies of silica-containing anatase have been made on materials synthesized at low temperature by sol-gel type methods (Yoshinaka et al. 1997; Okada et al. 2001) or at high temperature by gas-phase reactions (Akhtar et al. 1992). Such processes usually produce nano-sized, non-equilibrated particles that give very broad X-ray diffraction lines or that may even remain amorphous until annealed. For gas-phase anatase, very small increases in unit-cell parameters with silica addition were found (Akhtar et al. 1992), while for sol-gel anatase, slight reductions in unit-cell parameters with silica addition were noted (Yoshinaka et al. 1997; Okada et al. 2001). In both cases, shifts in the X-ray peaks do suggest some kind of compositional change

with increased SiO_2 in the reaction system, but exactly what this is, and how much Si is actually in the anatase, are not well constrained. Unit-cell size reductions suggested the possibility of ^{VI}Si formation (Okada et al. 2001). However, ^{29}Si NMR (Okada et al. 2001) detected only very broad ^{IV}Si peaks with chemical shifts of about –90 to –115 ppm and no ^{VI}Si (detection limits with isotopically normal Si were likely to be at least a few percent). These shifts are not consistent with isolated ^{IV}Si sites in the rutile (Q^0), but were more likely due to a residual high-silica amorphous phase. It seems unlikely that Si substitution into interstitial sites could reach the suggested 10–15 wt% level, especially given the ^{IV}Si content found here for 1 bar rutile that is about 1000× less. In any case, low-temperature or gas-phase anatase samples are unlikely to represent equilibrium solid solutions. In contrast, the chemical shift of –77.3 ppm found here for ^{IV}Si in rutile is in the range that would be expected for Q^0 sites with relatively high-charged cation neighbors in octahedral or higher coordination (Stebbins 1995).

Recent ^{27}Al NMR studies of ^{VI}Al dissolved in stishovite and rutile allow some interesting comparisons of the complexities of local structural effects on chemical shifts of such minor substituents. In stishovite synthesized at 1450 °C and 13 GPa with excess H_2O, Al is present in relatively symmetrical octahedral sites that are apparently not directly paired with oxygen vacancies, and which have isotropic chemical shifts of +11 ppm (Stebbins et al. 2006), near the high end of the known range for ^{VI}Al in oxides. At least at low Al concentrations in material equilibrated at 1400 to 1500 °C, Al in rutile also is found in symmetrical octahedral sites, with chemical shifts of about –6 ppm (Stebbins 2007), near the low end of the known range. At higher concentrations, other types of Al sites become important. This difference can be attributed (Stebbins 2007) to the much longer expected cation-oxygen distances in rutile, i.e., the mean Ti-O distance in rutile of 1.96 Å vs. the mean Si-O distance in stishovite of 1.78 Å (Smyth and Bish 1988). In contrast, the chemical shift for ^{VI}Si in stishovite (–191.2 ppm) is much lower than that observed here for ^{VI}Si in rutile (–177.5 ppm). In this case, a second-neighbor effect of the much higher electronegativity of Si vs. Ti may be predominant, or perhaps the direction of the chemical shift change is reversed by a difference in the way that the rutile and stishovite structures locally relax to accommodate either cation size or charge mismatch.

^{VI}Si in TiO_2-II has only slightly different chemical shifts from this species in rutile and shows as well a split peak (–174.0 and –176.0 ppm). The latter is not expected from the single Ti site in the structure (Filatov et al. 2007). Given that the mean Ti-O bond distance of 1.97 Å is only slightly greater than that for rutile (1.96 Å), and that the connectivity of the octahedra in the two structures is similar, the similarity of the chemical shifts is not surprising. However, the lower symmetry of TiO_2-II (orthorhombic vs. tetragonal for rutile) might allow it to relax in a more complex way to accommodate the much smaller Si^{4+} cation, perhaps leading to Si sites with two slightly different local environments and producing the observed NMR peak splitting. Or, the response of SiO_2-containing TiO_2-II to quench or decompression could be different from that of rutile. For both phases, future theoretical calculations would be very useful to connect such details of shifts with structure.

Acknowledgments

This work was supported by the NSF, grant no. EAR-04-08410 to J. Stebbins. We thank Edward Stolper and Paul Asimow for discussions that inspired us to conduct this study. Brian Balta graciously helped with EPMA. We are grateful for the helpful comments of two anonymous reviewers.

References cited

Akhtar, M.K., Pratsinis, S.E., and Mastrangelo, S.V.R. (1992) Dopants in vapor-phase synthesis of titania powders. Journal of the American Ceramic Society, 75, 3408–3416.

Filatov, S.K., Bendeliani, N.A., Albert, B., Kopf, J., Dyuzheva, T.I., and Lityagina, L.M. (2007) Crystalline structure of the TiO_2 II high-pressure phase at 293, 223, and 113 K according to single-crystal X-ray diffraction data. Doklady Physics, 52, 195–199.

Gaetani, G.A., Asimow, P.D., and Stolper, E.M. (2008) A model for rutile saturation in silicate melts with applications to eclogite partial melting in subduction zones and mantle plumes. Earth and Planetary Science Letters, 272, 720–729.

Grey, C.P., Smith, M.E., Cheetham, A.K., Dobson, R., and Dupree, R. (1990) Y-89 MAS NMR study of rare-earth pyrochlores-paramagnetic shifts in the solid state. Journal of the American Chemical Society, 112, 4670–4680.

Hartman, J.S., Narayanan, A., Rigby, S.S., Sliwinski, D.R., Halden, N.M., and Bain, A.D. (2007) Heterogeneities in sol-gel-derived paramagnetics-doped forsterites and willemites-electron microprobe analysis and stretched-exponential ^{29}Si NMR spin-lattice relaxation studies. Canadian Journal of Chemistry, 85, 56–65.

Johnson, O.W., Paek, S.-H., and Deford, J.W. (1975) Diffusion of H and D in TiO_2: Suppression of internal fields by isotope exchange. Journal of Applied Physics, 46, 1026–1033.

Kelsey, K.E., Stebbins, J.F., Mosenfelder, J.L., and Asimow, P.D. (2009) Simultaneous aluminum, silicon, and sodium coordination changes in 6 GPa sodium aluminosilicate glasses. American Mineralogist, 94, 1205–1215.

Khomenko, V.M., Langer, K., Rager, H., and Gett, A. (1998) Electronic absorption by Ti^{3+} ions and electron delocalization in synthetic blue rutile. Physics and Chemistry of Minerals, 25, 338–346.

Leinenweber, K., Mosenfelder, J., Diedrich, T., Soignard, E., Sharp, T.G., Tyburczy, J.A., and Wang, Y. (2006) High-pressure cells for in situ multi-anvil experiments. High Pressure Research, 26, 283–292.

MacKenzie, K.J.D. and Smith, M.E. (2002) Multinuclear Solid-State NMR of Inorganic Materials, 727 p. Pergamon, New York.

McQueen, R.G., Jamieson, J.C., and Marsh, S.P. (1967) Shock-wave compression and X-ray studies of titanium dioxide. Science, 155, 1401–1404.

Moore, D.K., Cherniak, D.J., and Watson, E.B. (1998) Oxygen diffusion in rutile from 750 to 1000 °C and 0.1 to 1000 MPa. American Mineralogist, 83, 700–711.

Mosenfelder, J.L., Deligne, N.I., Asimow, P.D., and Rossman, G.R. (2006) Hydrogen incorporation in olivine from 2–12 GPa. American Mineralogist, 91, 285–294.

Mposkos, E.D. and Kostopoulos, D.K. (2001) Diamond, former coesite and supersilicic garnet in metasedimentary rocks from the Greek Rhodope: A new ultrahigh-pressure metamorphic province established. Earth and Planetary Science Letters, 192, 497–506.

Okada, K., Yamamoto, N., Kameshima, Y., Yasumori, A., and MacKenzie, K.J.D. (2001) Effect of silica additive on the anatase to rutile phase transition. Journal of the American Ceramic Society, 84, 1591–1596.

Phillips, B.L., Thompson, J.G., Xiao, Y., and Kirkpatrick, R.J. (1993) Constraints on the structure and dynamics of the β-cristobalite polymorphs of SiO_2 and $AlPO_4$ from ^{31}P, ^{27}Al and ^{29}Si NMR spectroscopy to 770 K. Physics and Chemistry of Minerals, 20, 341–352.

Ren, Y., Fei, Y., Yang, J., and Bai, W. (2009) SiO_2 solubility in rutile at high temperature and high pressure. Journal of Earth Science, 20, 274–283.

Schulze, D.J. (1990) Silicate-bearing rutile-dominated nodules from South African kimberlites: metasomatized cumulates. American Mineralogist, 75, 97–104.

Smith, J.V. and Blackwell, C.S. (1983) Nuclear magnetic resonance of silica polymorphs. Nature, 303, 223–225.

Smyth, J.R. and Bish, D.L. (1988) Crystal Structures and Cation Sites of the Rock-Forming Minerals, 332 p. Allen and Unwin, Boston.

Spearing, D.R., Farnan, I., and Stebbins, J.F. (1992) Dynamics of the α–β phase transitions in quartz and cristobalite as observed by in situ high temperature ^{29}Si and ^{17}O NMR. Physics and Chemistry of Minerals, 19, 307–321.

Stebbins, J.F. (1992) Nuclear magnetic resonance spectroscopy of geological materials. Materials Research Society Bulletin, 17, 45–52.

——— (1995) Nuclear magnetic resonance spectroscopy of silicates and oxides in geochemistry and geophysics. In T.J. Ahrens, Eds., Handbook of Physical Constants, p. 303–332. American Geophysical Union, Washington, D.C.

——— (2007) Aluminum substitution in rutile titanium dioxide: new constraints from high-resolution ^{27}Al NMR. Chemistry of Materials, 19, 1862–1869.

Stebbins, J.F. and Kanzaki, M. (1990) Local structure and chemical shifts for six-coordinated silicon in high-pressure mantle phases. Science, 251, 294–298.

Stebbins, J.F. and Kelsey, K.E. (2009) Anomalous resonances in ^{29}Si and ^{27}Al NMR spectra of pyrope ($[Mg,Fe]_3Al_2Si_3O_{12}$) garnets: effects of paramagnetic cations. Physical Chemistry Chemical Physics, 11, 6906–6917.

Stebbins, J.F., Du, L.-S., Kelsey, K., Kojitani, H., Akaogi, M., and Ono, S. (2006) Aluminum substitution in stishovite and $MgSiO_3$ perovskite: High-resolution ^{27}Al NMR. American Mineralogist, 91, 337–343.

Stebbins, J.F., Smyth, J.R., Panero, W.R., and Frost, D.J. (2009) Forsterite, hydrous, and anhydrous wadsleyite and ringwoodite (Mg_2SiO_4): ^{29}Si NMR results for chemical shift anisotropy, spin-lattice relaxation, and mechanism of hydration. American Mineralogist, 94, 905–915.

Tse, D. and Hartmann, S.R. (1968) Nuclear spin-lattice relaxation via paramagnetic centers without spin diffusion. Physical Review Letters, 21, 511–514.

Vinograd, V.L., Wilson, D.J., and Winkler, B. (2008) Thermodynamics of mixing in rutile-stishovite solid solutions from quantum-mechanical calculations. 9th International Kimberlite Conference, Abstract no. 9IKC-A-00257.

Withers, A.C., Essene, E.J., and Zhang, Y. (2003) Rutile/TiO_2 II phase equilibria. Contributions to Mineralogy and Petrology, 145, 199–204.

Yang, J., Dobrzhinetskaya, L., Bai, W., Fang, Q., Robinson, P.T., Zhang, J., and Green, H.W. (2007) Diamond- and coesite-bearing chromitites from the Luobosa ophiolite, Tibet. Geology, 35, 875–878.

Yang, J.S., Bai, W.J., Fang, Q.S., Yan, B., Shi, N., Ma, Z., Dai, M., and Xiong, M. (2003) Silicon-rutile: an ultrahigh pressure (UHP) mineral from an ophiolite. Progress in Natural Science, 13, 528–531.

Yoshinaka, M., Hirota, K., and Yamaguchi, O. (1997) Formation and sintering of TiO_2 (anatase) solid solution in the system TiO_2-SiO_2. Journal of the American Ceramic Society, 80, 2749–2753.

Zack, T., Moraes, R., and Kronz, A. (2004) Temperature dependence of Zr in rutile: empirical calibration of a rutile thermometer. Contributions to Mineralogy and Petrology, 148, 471–488.

Manuscript received January 5, 2010
Manuscript accepted March 9, 2010
Manuscript handled by Lars Ehm